MACROPOROUS $PDMS_{STAR}$–MA:PEG-DA HYDROGELS FOR OSTEOCHONDRAL REGENERATION

An Undergraduate Research Scholars Thesis

by

REBECCA SEHNERT

Submitted to the Undergraduate Research Scholars program
Texas A&M University
in partial fulfillment of the requirements for the designation as an

UNDERGRADUATE RESEARCH SCHOLAR

Approved by
Research Advisor: Dr. Melissa Grunlan

May 2016

Major: Biomedical Engineering

TABLE OF CONTENTS

ABSTRACT

Macroporous $PDMS_{star}$–MA:PEG-DA Hydrogels for Osteochondral Regeneration

Rebecca Sehnert
Department of Biomedical Engineering
Texas A&M University

Research Advisor: Dr. Melissa Grunlan
Department of Biomedical Engineering

Osteochondral defects (OCDs) are the result of severe cartilage loss leading to exposure and damage of the subchondral bone. “Materials-guided” tissue engineering is a promising approach to treat these defects, in which a scaffold may mediate the process of OCD regeneration via instructive and tunable physical and chemical properties. For effective healing, an ideal scaffold would spatially direct tissue to mimic the native transition of the osteochondral interface. Conventional poly(ethylene glycol) diacrylate (PEG-DA) hydrogels prepared using aqueous precursor solutions have been commonly studied for tissue engineering purposes, but lack a wide range of desired chemical and physical properties. This study will seek to develop a superior PEG-DA scaffold for OCD repair by (1) integrating methacrylated star polydimethylsiloxane ($PDMS_{star}$-MA) to increase bioactivity and osteoinductivity, (2) employing solvent induced phase separation (SIPS) with the use of an organic solvent, and (3) incorporating salt leaching techniques to achieve an interconnected network of pores to allow for cell infiltration. Total macromer concentration (20, 30, and 40 wt%), ratio of $PDMS_{star}$-MA to PEG-DA (0:100 and 20:80 wt%), and average salt particle size will be studied with regard to their impact on scaffold morphology, swelling, mechanical properties, and degradation. The tunable nature of these hydrogels could prove especially useful to study material-guided cell behavior for the purpose of osteochondral tissue regeneration.

ACKNOWLEDGMENTS

I would like to acknowledge Dr. Melissa Grunlan, Erica Gacasan, and Daniel Ehrhardt for their indispensable help on this work.

NOMENCLATURE

MSC	Mesenchymal stem cell
OCD	Osteochondral defect
$PDMS_{star}$-MA	Methacylated star polydimethylsiloxane
PEG-DA	Poly(ethylene glycol) diacrylate
ROP	Regenerative osteochondral plug
SIPS	Solvent induced phase separation
SCPL	Solvent casting/Particulate leaching
wt %	Weight percent

CHAPTER I

INTRODUCTION

Osteochondral defects (OCDs) are injuries defined by an advanced state of cartilage loss, leading to the exposure and subsequent damage of the subchondral bone [1, 2]. These defects result in high incidences of joint pain and disability, and can often lead to osteoarthritis, immobility, and even total join replacement [3]. Due to the limited vasculature of articular cartilage, OCDs are extremely restricted in terms of their ability to self-repair [1, 4]. This process is complicated by the abating mechanical support of the defect region as the subchondral cancellous bone is subject to further damage. Due to major shortcomings in current clinical repair strategies such as autografting and total joint replacement, a "materials-guided" tissue engineering approach is proposed in which the tunable physical and chemical properties of an instructive, biodegradable scaffold can direct cell healing [5, 6]. To mimic the native osteochondral interface, this instructive scaffold must spatially direct regeneration of tissues spanning from articular cartilage to cancellous bone. To achieve this end, a gradient of physical (morphology, modulus) and chemical (bioactivity, hydration, and hydrophobicity) properties is needed to properly direct cell differentiation and proliferation [7, 8]. Using this approach, regeneration of tissues with properties similar to the native osteochondral interface may be accomplished.

Previously, conventional poly(ethylene glycol) diacrylate (PEG-DA) hydrogels prepared from aqueous precursor solutions have been commonly studied for tissue regeneration applications [5, 7, 9, 10]. These hydrogels serve as "biological blank slates," meaning that they resist protein absorption and undesired cell adhesion to allow for the controlled introduction of desired cells

[11-13]. However, conventional PEG-DA hydrogels have a very limited range of physical and chemical properties, including a lack of bioactivity and osteoinductivity, as well as a lack of tunable morphology [11, 12]. To supplement these hydrogels, it has been previously shown that the incorporation of methacrylated star polydimethylsiloxane ($PDMS_{star}$-MA) leads to an increased range of physical and chemical properties [12]. The inorganic, hydrophobic $PDMS_{star}$-MA was shown to increase osteoinductivity and prompt the differentiation of mesenchymal stem calls (MSCs) into osteoblasts in proportion to the macromer concentration [11-13]. Subsequently, it was shown that these effects could be enhanced through the employment of solvent induced phase separation (SIPS), in which an organic solvent was used rather than the traditional aqueous solvent [11, 12]. These hybrid PDMSstar-MA:PEG-DA scaffolds were shown to exhibit increased modulus, pore size, and degradation rates than corresponding scaffolds fabricated from aqueous precursor solutions, as well as a more uniform distribution of $PDMS_{star}$-MA [11, 12].

One key shortcoming of SIPS protocols is that due to the use of an organic solvent, cells cannot be directly photoencapsulated during fabrication as is done with conventional hydrogels. This necessitates the post-fabrication seeding of cells into the hydrogel via pores. Thus, it is critical that an interconnected network of pores be present in the hydrogel for this system to be viable for tissue engineering purposes. In addition, these macroporous networks of pores have been shown to assist tissue regeneration by enhancing neotissue formation and cell integration, as well as facilitating the diffusion of cell nutrients and wastes [14-17]. Furthermore, it has been shown that there is an optimal scaffold pore size corresponding to the regeneration of specific tissues. Relevant to the regeneration of OCDs, the optimal pore size for cancellous bone regeneration is

100-450 μm [18, 19], while 100-200 μm [18] is desired for cartilage. Several methods have been previously investigated for the incorporation of macroporous morphologies into conventional PEG-DA hydrogels including gas foaming [16], cryogelation [9, 14], and particulate leaching [15, 20]. However, the use of these techniques remains limited due to the need for specialized equipment or extreme temperatures.

In this study, a salt leaching fabrication protocol will be incorporated into hybrid $PDMS_{star}$-MA:PEG-DA hydrogels in order to create macroporous morphologies. This approach has seen limited use in conventional scaffolds due to their use of aqueous precursor solutions, but is made possible in this case through the SIPS protocol [15, 21]. Hydrogel series of increasing macromer wt % and ratio of $PDMS_{star}$-MA to PEG-DA will be fabricated, and the effectiveness of a modified solvent casting particulate leaching (SCPL) technique to create macroporous morphologies evaluated. The resultant hydrogel properties of equilibrium swelling, storage modulus, and degradation will also be evaluated for each composition.

CHAPTER II

METHODS

Materials

Tetrakis(dimethylsiloxy)silane (tetra-SiH), octamethylcyclotetrasiloxane (D_4), and Pt-divinyltetramethyldisiloxane complex (Karstedt's catalyst, 2wt.% in xylene) were obtained from Gelest. Hexamethyldisilazane (HMDS), acryloyl chloride, allyl methacrylate, poly(ethylene glycol) (PEG; PEG-3400, MW=3000-3700 g mol-1 per manufacturers specifications), triethylamine (Et_3N), triflic acid, 1-vinyl-2-pyrrolidinone (NVP), 2,2-dimethyl-2-phenyl-acetophenone (DMAP), K_2CO_3, $MgSO_4$, NaOH, NaCl and solvents were obtained from Sigma. High-performance liquid chromatography grade toluene, dichloromethane (CH_2Cl_2), and NMR grade chloroform ($CDCl_3$) were obtained from Sigma and dried over molecular sieves. NaCl was sifted (A. S. T. M. E-11 Specification, No. 40, 425 μm opening; No.60, 250 μm opening) to obtain an average salt size of 459 ± 69 μm (LS), 268 ± 35 μm (MS), and 181 ± 29 μm (SS). These salt sizes had been previously calculated from SEM images analyzed with ImageJ® software [22].

Methods

PEG-DA synthesis

3.4k PEG-DA was synthesized as previously reported. PEG-3400 (23.5 g, 7.0 mmol), Et_3N (1.95 ml, 14.0 mmol) and acryloyl chloride (2.27 ml, 28.0 mmol) were reacted under N_2 atmosphere overnight to obtain PEG-DA. The product was washed with K_2CO_3, then precipitated in ether

and dried under reduced pressure (14.7 psi) (17.1 g, 70% yield). 1H-NMR end-group analysis verified the M_n of the resultant PEG-DA to be 3393 g mol-1 (~3400 g mol^{-1}) [12].

$PDMS_{star}$-MA synthesis

$PDMS_{star}$-MA was prepared as previously reported [23]. Tetra-SiH (1.1 g, 3.3 mmol), D_4 (29.9 g, 100.8 mmol), and triflic acid (60 µl) were reacted under N_2 overnight and neutralized with HMDS (.15 g, .93 mmol) to obtain colorless, liquid $PDMS_{star}$-SiH (24.8 g, 83%). Next, $PDMS_{star}$-SiH (20.0 g, 2.9 mmol) was reacted with allyl methacrylate (1.6 g, 12.7 mmol), toluene (35 ml), and Karstedt's catalyst (100 µl) under N_2 for 12 hours at 90ºC. The resultant product was purified via flash column chromatography to obtain $PDMS_{star}$-MA (12.6 g, 63% yield).

NMR

1H-NMR spectra were obtained on a Mercury 300 300 MHz spectrometer operating in the Fourier transform mode. Five percent (w/v) $CDCl_3$ solutions were used to obtain spectra. Residual $CHCl_3$ served as an internal standard.

Hydrogel preparation

Cylindrical, macroporous hydrogel scaffolds were fabricated through a multistep process involving the creation of a sacrificial salt template around which a polymer solution then was crosslinked to form a hydrogel. The sacrificial template was fabricated by placing 3.0 g of a 5 wt% water to sized NaCl mixture into glass vial (OD = 15 mm). This template was centrifuged (10 min, 4000 rpm) to evenly distribute and fuse salt, and was dried overnight at room temperature (RT). Precursor solutions were then prepared in DCM at concentrations of 20, 30

and 40 wt% total macromer to total mass of solution, and at wt% rations of 0:100 (pure) and 20:80 (hybrid) $PDMS_{star}$-MA to PEG-DA. Photocatalyst (30 wt% DMAP in NVP) was added at a ratio of 10 µl per ml of solution, and the precursor solution added to cover the salt template (~ 1 ml). The sealed vial was centrifuged (5 min, 2000 rpm) to distribute solution and subsequently cured via exposure to UV light for 6 minutes (UV-transilluminator, 6 mW cm^{-2}, 365 nm). After air drying overnight to remove solvent, the construct was removed from the vial and cross-sectioned to 1.2 mm width using a vibratome (Leica VT 1000 S). The slabs were leached by soaking in DI water on a rocker table (100 rpm) for 48 hr to remove salt and any impurities, as well as to allow for swelling of the hydrogel disks (15 mm diameter, 1.8 mm height). This process is depicted below in Figure 1.

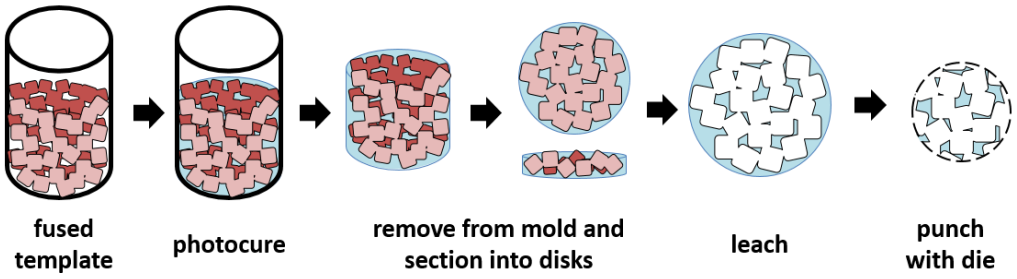

Figure 1: Adapted solvent-casting/particulate leaching (SCPL) technique used to create macroporous hydrogel scaffolds. Salt fusion was achieved using a 5 wt% water to NaCl mixture. The hydrogel precursor solution then was photocured around the salt template, sectioned into disks, and leached.

Additionally, non-porous hydrogel slabs were fabricated as previously reported [12]. Precursor solutions were prepared as above, pipetted between two clamped microscope slides (75 x 50 mm) separated by Teflon spacers (1.5 mm thick), and exposed to UV light for 6 min to create planar non-porous hydrogel sheets. Hydrogel sheets were removed from the mold, air dried for

30 min, and then soaked in DI water for 48 hrs at 100 rpm to allow for swelling and removal of impurities. All hydrogel samples were permitted to soak in DI water for 48 hr prior to testing.

Scanning electron microscopy

Water swollen hydrogel samples (8 mm diameter) were flash frozen in liquid nitrogen for 1 min and then immediately lyophilized for 24 hr (Labconoco Centri Vap, Gel Dryer System). Specimen cross sections underwent Pt-sputter coating and were viewed using a field emission scanning electron microscope (JEOL JCM-5000) at an accelerated electron energy of 15 keV.

Percent porosity

For each porated composition, as well as the corresponding non-porated slabs, five samples (8mm diameter) were punched with a die. Excess water was removed and the samples were dried under vacuum (14.7 psi, 60 ºC, 24 hr), after which their dry weight ($W_{D(porous)}$, $W_{D(non\text{-}porous)}$) was measured. The percent porosity (%P) of the hydrogel samples was defined as below.

Equation 1: $$\% P = (W_{D(non\text{-}porous)} - W_{D(porous)}) / W_{D(non\text{-}porous)} * 100$$

Equilibrium swelling ratio

For each composition, three samples (8 mm diameter) were punched from porated hydrogel discs with a die. Each sample was placed in a sealed scintillation vial with 10 ml DI water on a rocker table (250 rpm) for 48 hours. Samples were removed and the water-swollen hydrogel weighed (W_S). Each sample was then dried under vacuum (14.7 psi, 60ºC, 24 hr) and the weight of the dried specimen taken (W_D). The swelling ratio is defined as below.

Equation 2: $\text{Swelling Ratio} = (W_S - W_D) / W_D$

Dynamic mechanical analysis

For each composition, three samples (8 mm diameter) were punched from porated hydrogel discs with a die. The storage modulus (G′) of each sample was measured in compression mode using a dynamic mechanical analyzer (TA Instruments Q800) equipped with a parallel-plate compression clamp, diameter ranging from 40 mm (bottom) to 15 mm (top). Each hydrated sample was clamped between the parallel plates and was tested in a multi-frequency strain mode (1-30 Hz) with amplitude of 10 μm and pre-load force of 0.1 N.

Degradation

For each composition, six samples (8 mm diameter) were punched from porated hydrogel discs with a die. After soaking in DI water for 3 hr, the initial swollen weight (W_0) was taken. Three samples were each placed into a well of a 24-well plate containing 1 ml 0.05 M NaOH, and the well plate covered with foil and incubated at 37ºC on a rocker table (100 rpm). The NaOH solution was exchanged every 12 hr, and swollen weights were recorded at regular intervals until the hydrogel exhibited a loss in swelling. The time required for each sample to completely dissolve was recorded.

Statistical Analysis

All data results are reported as the mean ± standard deviation. For each set of data, mean values were compared using ANOVA followed by a Tukey *post hoc* test in which a p-value <0.05 was considered statistically different.

CHAPTER III

RESULTS

Hydrogel fabrication

Due to its ease of application and ability to effectively control pore size through porogen selection, an adapted solvent-casting/particulate leaching (SCPL) protocol was employed [24, 25]. This method was especially well suited for hydrogels fabricated using SIPS, as the NaCl porogen was not soluble in the DCM solvent used. By the addition of 5 wt% water to the NaCl particles to partially dissolve the discrete crystals and form a continuous template, high interconnectivity of pores was obtained [22]. Photopolymerization of DCM based $PDMS_{star}$-MA: PEG-DA precursor solution around this template and subsequent leaching of the salt yielded spongy scaffolds with visible porosity.

Hydrogel morphology

Recently, hybrid $PDMS_{star}$-MA: PEG-DA hydrogels were fabricated via SIPS involving a DCM precursor solution without the use of a sacrificial porogen template, and enhanced pore size was shown in compositions containing high levels of $PDMS_{star}$-MA [12]. This is due to the separation of the growing polymer chains into polymer-rich and polymer-lean domains (i.e. pores) during the SIPS process. The porosity and physical structure of a scaffold has been shown to influence and direct cell behavior and differentiation by mimicking the properties of native ECM. Pore size and interconnectivity are vital properties in a scaffold to ensure cell seeding efficiency and cell penetration [26], while also aiding in molecular transport of cell nutrients, wastes, and biological

chemicals. While SIPS enhanced the porosity of hybrid $PDMS_{star}$-MA: PEG-DA hydrogels, the scaffolds still lacked this high level of interconnectivity.

To address this shortcoming, $PDMS_{star}$-MA: PEG-DA hydrogels were prepared using a sacrificial salt template composed of porogen sizes of 181 ± 29 μm (SS), 268 ± 35 μm (MS), and 459 ± 69 μm (LS). After leaching in DI water, highly porous interconnected matrixes that could be visually observed under normal light were observed. There was no visible difference between constructs containing $PDMS_{star}$-MA verses those constructed of pure PEG-DA or constructs of varying macromer concentrations, although templates with varying salt sizes were easily distinguishable, as seen in Figure 2.

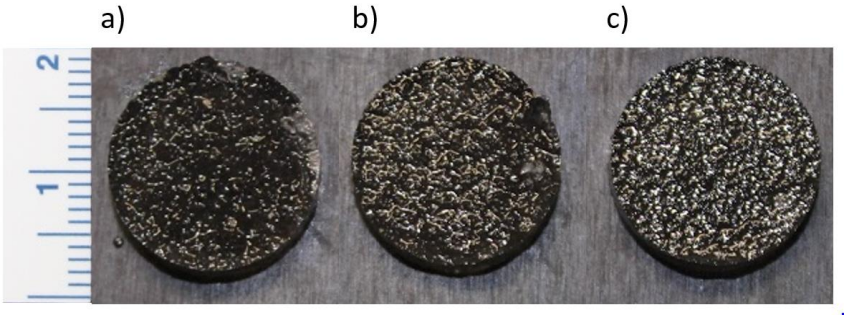

Figure 2: Macroscopic images showing effect of porogen size on hydrogel morphology. Polymer composition of 30 wt% (0:100) $PDMS_{star}$-MA:PEG-DA consistent for all hydrogels. a) Large salt porogen b) Medium salt porogen c) Small salt porogen.

The morphologies of the hydrogel scaffolds were examined using SEM, as shown in Figure 3. The SEM images of hydrogel cross sections verify a high degree of interconnected porosity for both the pure and hybrid samples, with pore size consistent with the geometry of NaCl particles used. There was no observed difference in samples with or without $PDMS_{star}$-MA.

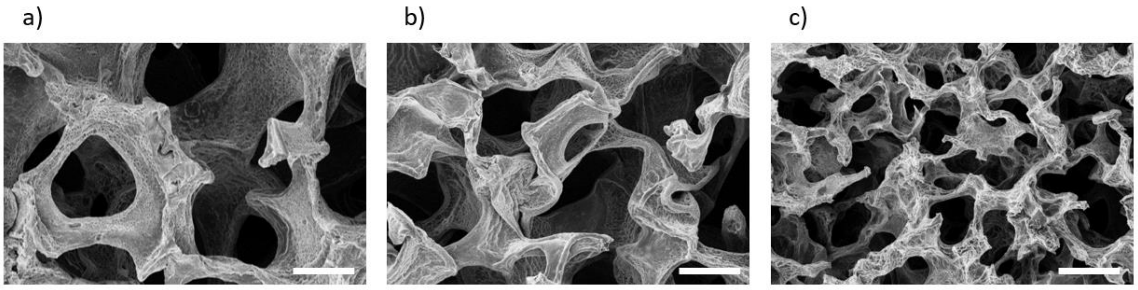

Figure 3: SEM images showing effect of porogen size on hydrogel morphology. Polymer composition of 30 wt% (0:100) $PDMS_{star}$-MA:PEG-DA consistent for all hydrogels. Scale bars shown indicate 200μm. a) Large salt porogen b) Medium salt porogen c) Small salt porogen.

To examine any differences due to macromer concentration, $PDMS_{star}$-MA content, or pore size, the overall porosity for each composition was determined. Figure 4 illustrates that differences in porosity among all of the compositions tested were observed to be statistically insignificant ($P>0.05$). This indicated that the introduction of macroporous morphologies through the SIPS/SCPL method has decoupled porosity from $PDMS_{star}$-MA content, total macromer concentration, and porogen size. This constant porosity may be a result of the constant packing faction of porogen per unit volume of scaffold across all compositions. These methods thus present an opportunity to investigate scaffold material properties independent of pore size.

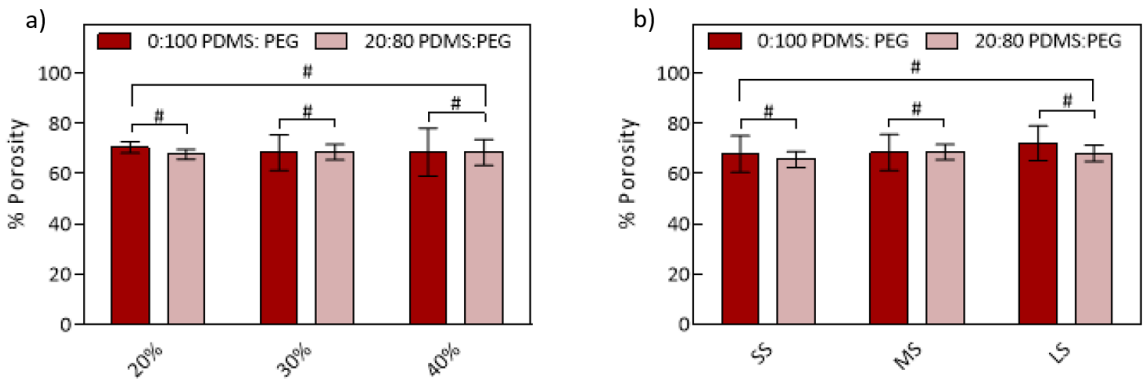

Figure 4: Scaffold properties of porosity as a function of macromer concentration and porogen size. a) Porosity over variable macromer concentration. b) Porosity over variable porogen size. Statistical significance was determined by two-way ANOVA, where * indicates $p < 0.05$ and # indicates $p > 0.05$.

Equilibrium swelling

The expansive swelling a hydrogel exhibits in aqueous environments is essential in mimicking the hydrated properties of the ECM, impacting the cellular environment, as well as affecting the diffusion of nutrients and wastes to the cells [5, 27]. To quantify this property, equilibrium swelling studies were conducted examine differences in scaffold hydration due to $PDMS_{star}$-MA content, macromer concentration, and pore size. Although the incorporation of $PDMS_{star}$-MA increases scaffold hydrophobicity, hybrid hydrogel compositions presented no difference in swelling ratios compared to pure PEG-DA samples (Figure 5a). This is attributed to the effects of the macroporous morphology overwhelming any changes in micro-architecture caused by incorporation of $PDMS_{star}$-MA. Also, it was shown that enhanced rigidity due to increasing macromer concentration led to a corresponding decrease in swelling ratios. This effect was observed to stabilize at higher wt% compositions, as the effects of enhanced rigidity on water uptake is opposed by the macroporous structure consistent with all compositions. In addition, it was shown that swelling ratio was decoupled from pore size (Figure 5b), which is attributed to the constant porosity (%P) across all compositions.

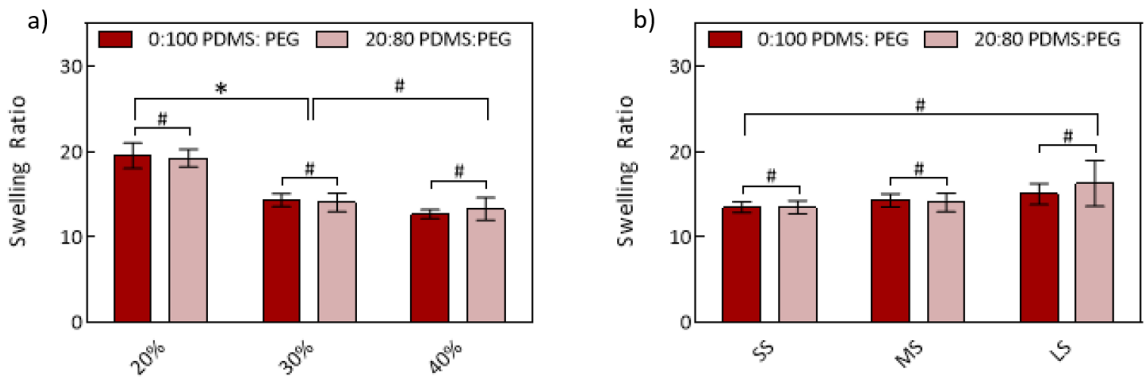

Figure 5: Scaffold properties of swelling ratio as a function of macromer concentration and porogen size. a) Equilibrium swelling over variable macromer concentration. b) Equilibrium swelling over variable porogen size. Statistical significance was determined by two-way ANOVA, where * indicates $p < 0.05$ and # indicates $p > 0.05$.

Modulus

Hydrogel stiffness, as defined by compressive storage modulus, is a measure used to determine many mechanical properties of hydrogels, and is known to affect cell behavior [27]. DMA was used to measure modulus as a function of frequency of the applied strain in compression. Following trends observed in swelling, $PDMS_{star}$-MA was observed to have no effect on modulus (Figure 6), which is again attributed to the higher effect of macroporous morphologies rather than $PDMS_{star}$-MA micro-architecture. Likewise, enhanced rigidity associated with increased total macromer concentration initially led to an increase in modulus, but again stabilized as wt% continued to increase due the opposing effect of macroporosity. When comparing modulus across pore sizes, an increase in compressive modulus was observed as pore size decreased (Figure 6b). This increase may be due to enhanced distribution of compressive forces and greater chain interactions within the matrix due to the smaller distances between pore walls.

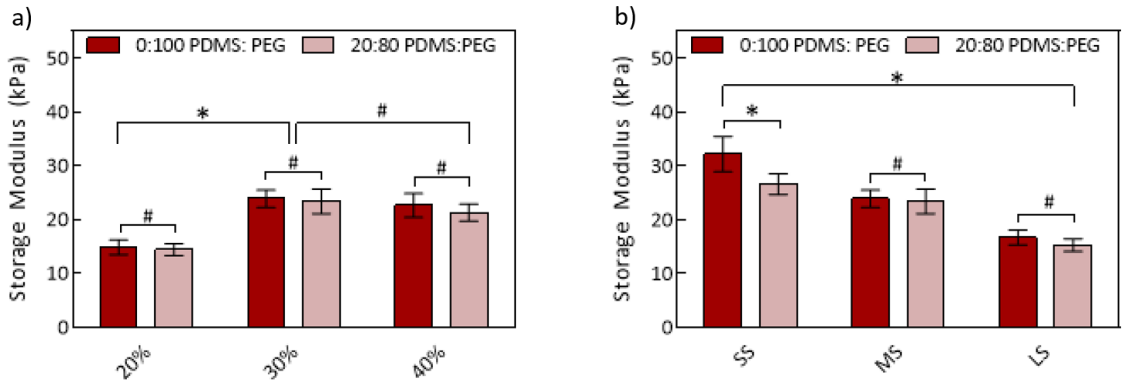

Figure 6: Scaffold properties of modulus as a function of macromer concentration and porogen size. a) Modulus over variable macromer concentration. b) Modulus over variable porogen size. Statistical significance was determined by two-way ANOVA, where * indicates $p < 0.05$ and # indicates $p > 0.05$.

Degradation

Hydrogel disks were subjected to hydrolytic degradation under accelerated basic conditions. The time to complete dissolution was determined with respect to macromer concentration, $PDMS_{star}$-MA, and pore size. Aliphatic polyesters exhibit an enhanced rate of hydrolytic degradation due to an autocatalytic effect caused by the slower diffusion of acidic degradation products through the thicker pore walls caused by larger pore sizes. Likewise, in PEG-DA based hydrogels the hydrolysis of ester bonds releases poly(acrylic acid) (PAA), and larger pore walls created through the incorporation of PDMSstar-MA have been shown to enhance degradation rates. However, these results are seen in scaffolds which lack an interconnected network of macroporosity. In the hydrogel scaffolds fabricated in this study, it was shown that pore size rather than $PDMS_{star}$-MA content was the main detriment to dissolution time (Figure 7). Increased pore sizes led to a decrease in degradation time due to the faster diffusion of acidic byproducts through the scaffold. Additionally, the incorporation of $PDMS_{star}$-MA was not shown to have a significant effect on dissolution time. As expected, it was also shown that increased

macromer concentrations led to an increased dissolution time. Thus, the scaffold's degradation profile is dependent on both pore size and macromer concentration.

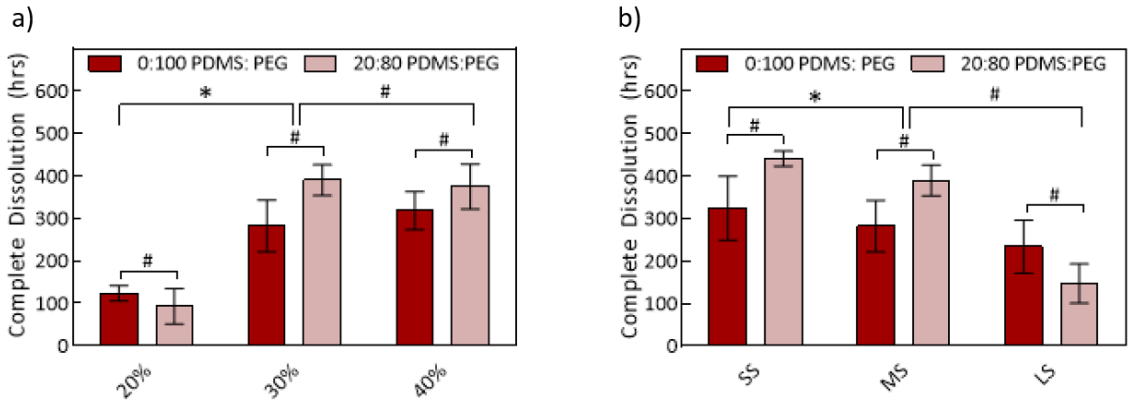

Figure 7: Scaffold properties of complete dissolution time under accelerated basic conditions as a function of macromer concentration and porogen size. a) Dissolution time over variable macromer concentration. b) Dissolution time over variable porogen size. Statistical significance was determined by two-way ANOVA, where * indicates $p < 0.05$ and # indicates $p > 0.05$.

CHAPTER IV

CONCLUSIONS

Improvement of PEG-DA hydrogels with enhanced physical and chemical properties such as bioactivity and interconnected porosity would serve especially useful in developing scaffold systems for OCD repair. Towards this end, this study proposed a hybrid $PDMS_{star}$-MA:PEG-DA scaffold to achieve bioactivity and osteoinductivity. The scaffolds were also fabricated via SIPS and SCPL methods to achieve high pore interconnectivity as well as tunable pore size. This allowed for the control of the scaffold's macroporous morphology.

The scaffold morphology, as demonstrated by pore size, was the main determinant of the resultant scaffold properties. An inverse relationship between effects of porosity and macromer concentration was observed, where the enhanced stiffness and reduced hydration of higher macromer concentrations was mitigated by larger pore sizes. It was also shown that the incorporation of $PDMS_{star}$-MA had minimal effects on scaffold morphology, stiffness, hydration, and degradation. These findings will allow for further investigation of cell-material interactions where chemistry ($PDMS_{star}$-MA content) is decoupled from the material properties of the scaffold. In addition, future studies will evaluate the extent to which $PDMS_{star}$-MA is covalently crosslinked within the hydrogel network by assessing varying curing protocol parameters (e.g. UV exposure time). Potential loss of uncrosslinked $PDMS_{star}$-MA will be evaluated by treating hydrogels with Nile Red to preferentially stain PDMS, followed by imaging with confocal microscopy.

In conclusion, the ability to tune the physical properties of these scaffolds by varying pore size, macromer concentration, and $PDMS_{star}$-MA content allows for a means to attain the interconnected pore architecture ideal for osteoblast formation. These tunable morphological, swelling, mechanical and degradation properties provide a necessary scaffold library to probe cell-material interactions and ultimately OCD healing.

REFERENCES

[1] D. J. Kelly and P. J. Prendergast, "Mechano-regulation of stem cell differentiation and tissue regeneration in osteochondral defects," *J Biomech,* vol. 38, pp. 1413-22, Jul 2005.

[2] S. Heir, T. K. Nerhus, J. H. Røtterud, S. Løken, A. Ekeland, L. Engebretsen, *et al.*, "Focal cartilage defects in the knee impair quality of life as much as severe osteoarthritis: a comparison of knee injury and osteoarthritis outcome score in 4 patient categories scheduled for knee surgery," *Am J Sports Med,* vol. 38, pp. 231-7, Feb 2010.

[3] P. M. Brooks, "The burden of musculoskeletal disease--a global perspective," *Clin Rheumatol,* vol. 25, pp. 778-81, Nov 2006.

[4] J. Gao, J. E. Dennis, L. A. Solchaga, V. M. Goldberg, and A. I. Caplan, "Repair of osteochondral defect with tissue-engineered two-phase composite material of injectable calcium phosphate and hyaluronan sponge," *Tissue Eng,* vol. 8, pp. 827-37, Oct 2002.

[5] J. L. Drury and D. J. Mooney, "Hydrogels for tissue engineering: scaffold design variables and applications," *Biomaterials,* vol. 24, pp. 4337-51, Nov 2003.

[6] N. P. Ziats, K. M. Miller, and J. M. Anderson, "In vitro and in vivo interactions of cells with biomaterials," *Biomaterials,* vol. 9, pp. 5-13, Jan 1988.

[7] B. M. Bailey, L. N. Nail, and M. A. Grunlan, "Continuous gradient scaffolds for rapid screening of cell-material interactions and interfacial tissue regeneration," *Acta Biomater,* vol. 9, pp. 8254-61, Sep 2013.

[8] K. Chatterjee, S. Lin-Gibson, W. E. Wallace, S. H. Parekh, Y. J. Lee, M. T. Cicerone, *et al.*, "The effect of 3D hydrogel scaffold modulus on osteoblast differentiation and mineralization revealed by combinatorial screening," *Biomaterials,* vol. 31, pp. 5051-62, Jul 2010.

[9] Y. Hwang, C. Zhang, and S. Varghese, "Poly(ethylene glycol) cryogels as potential cell scaffolds: effect of polymerization conditions on cryogel microstructure and properties," *Journal of Materials Chemistry,* vol. 20, pp. 345-351, 2010.

[10] Y. Hwang, N. Sangaj, and S. Varghese, "Interconnected macroporous poly(ethylene glycol) cryogels as a cell scaffold for cartilage tissue engineering," *Tissue Eng Part A,* vol. 16, pp. 3033-41, Oct 2010.

[11] B. M. Bailey, V. Hui, R. Fei, and M. A. Grunlan, "Tuning PEG-DA hydrogel properties via solvent-induced phase separation (SIPS)()," *J Mater Chem*, vol. 21, pp. 18776-18782, Jan 2011.

[12] B. M. Bailey, R. Fei, D. Munoz-Pinto, M. S. Hahn, and M. A. Grunlan, "PDMS(star)-PEG hydrogels prepared via solvent-induced phase separation (SIPS) and their potential utility as tissue engineering scaffolds," *Acta Biomater*, vol. 8, pp. 4324-33, Dec 2012.

[13] Y. Hou, C. A. Schoener, K. R. Regan, D. Munoz-Pinto, M. S. Hahn, and M. A. Grunlan, "Photo-cross-linked PDMSstar-PEG hydrogels: synthesis, characterization, and potential application for tissue engineering scaffolds," *Biomacromolecules*, vol. 11, pp. 648-56, Mar 2010.

[14] N. S. Hwang, C. Zhang, Y. S. Hwang, and S. Varghese, "Mesenchymal stem cell differentiation and roles in regenerative medicine," *Wiley Interdiscip Rev Syst Biol Med*, vol. 1, pp. 97-106, 2009 Jul-Aug 2009.

[15] Y. C. Chiu, J. C. Larson, A. Isom, and E. M. Brey, "Generation of porous poly(ethylene glycol) hydrogels by salt leaching," *Tissue Eng Part C Methods*, vol. 16, pp. 905-12, Oct 2010.

[16] A. Sannino, P. A. Netti, M. Madaghiele, V. Coccoli, A. Luciani, A. Maffezzoli, *et al.*, "Synthesis and characterization of macroporous poly(ethylene glycol)-based hydrogels for tissue engineering application," *J Biomed Mater Res A*, vol. 79, pp. 229-36, Nov 2006.

[17] J. H. Brauker, V. E. Carr-Brendel, L. A. Martinson, J. Crudele, W. D. Johnston, and R. C. Johnson, "Neovascularization of synthetic membranes directed by membrane microarchitecture," *J Biomed Mater Res*, vol. 29, pp. 1517-24, Dec 1995.

[18] P. Duan, Z. Pan, L. Cao, Y. He, H. Wang, Z. Qu, *et al.*, "The effects of pore size in bilayered poly(lactide-co-glycolide) scaffolds on restoring osteochondral defects in rabbits," *J Biomed Mater Res A*, vol. 102, pp. 180-92, Jan 2014.

[19] Y. Gong, Z. Ma, C. Gao, W. Wang, and J. Shen, "Specially elaborated thermally induced phase separation to fabricate poly(L-lactic acid) scaffolds with ultra large pores and good interconnectivity," *Journal of Applied Polymer Science*, vol. 101, pp. 3336-3342, 2006.

[20] C. W. Chen, M. W. Betz, J. P. Fisher, A. Paek, and Y. Chen, "Macroporous hydrogel scaffolds and their characterization by optical coherence tomography," *Tissue Eng Part C Methods*, vol. 17, pp. 101-12, Jan 2011.

[21] W. K. Lee, T. Ichi, T. Ooya, T. Yamamoto, M. Katoh, and N. Yui, "Novel poly(ethylene glycol) scaffolds crosslinked by hydrolyzable polyrotaxane for cartilage tissue engineering," *J Biomed Mater Res A*, vol. 67, pp. 1087-92, Dec 2003.

[22] D. Zhang, W. L. Burkes, C. A. Schoener, and M. A. Grunlan, "Porous inorganic-organic shape memory polymers," *Polymer (Guildf)*, vol. 53, pp. 2935-2941, Jun 2012.

[23] M. A. Grunlan, N. S. Lee, F. Mansfeld, E. Kus, J. A. Finlay, J. A. Callow, *et al.*, "Minimally adhesive polymer surfaces prepared from star oligosiloxanes and star oligofluorosiloxanes," *Journal of Polymer Science Part A: Polymer Chemistry*, vol. 44, pp. 2551-2566, 2006.

[24] A. G. Mikos, A. J. Thorsen, L. A. Czerwonka, Y. Bao, R. Langer, D. N. Winslow, *et al.*, "Preparation and characterization of poly (L-lactic acid) foams," *Polymer*, vol. 35, pp. 1068-1077, 1994.

[25] Y. Xie, S. Yang, and D. A. Kniss, "Three-dimensional cell-scaffold constructs promote efficient gene transfection: implications for cell-based gene therapy," *Tissue engineering*, vol. 7, pp. 585-598, 2001.

[26] F. J. O'Brien, B. Harley, I. V. Yannas, and L. J. Gibson, "The effect of pore size on cell adhesion in collagen-GAG scaffolds," *Biomaterials*, vol. 26, pp. 433-441, 2005.

[27] C. M. Kirschner and K. S. Anseth, "Hydrogels in healthcare: from static to dynamic material microenvironments," *Acta materialia*, vol. 61, pp. 931-944, 2013.